TECHNICAL UNIVERSITY OF CLUJ-NAPOCA

ACTA TECHNICA NAPOCENSIS

OPTIMIZATION OF ANN USED TO PREDICT THE SURFACE ROUGHNESS IN DRY TURNING OF UNS A97075 AERONAUTICAL ALUMINUM ALLOY

Ignacio REPISO-LÓPEZ, Sergio MARTÍN-BÉJAR,
Francisco Javier TRUJILLO, Lorenzo SEVILLA

Abstract: *In the present work, a prediction model of the surface roughness in the dry turning of UNS A97075 aeronautical aluminum alloy was developed using artificial neural network (ANN). Specifically, the cutting speed and feed rate influence on the maximum height of roughness profile has been analyzed, due to its influence in the fatigue behavior of machined parts. Furthermore, the effect of the network architecture, such as the optimal number of neurons in the hidden layer, and the selection of experimental results applied in the ANN's training and validation was studied to determine the best fit, minimizing the root mean square error. The use of ANNs has been shown to be a useful tool for such regression task, obtaining a high level of fit, even higher than the existing models in the literature in this regard.*
Keywords: *Surface Integrity, Surface Roughness, Artificial Neural Network, Optimization, Tuning Hyperparameters, Dry turning, Aluminum Alloys.*

1. INTRODUCTION

Aircraft industry is well known for being characterized by high requirements based on the reliability, effectiveness, quality, and safety manufacturing processes conditions. In this regard, research and development works have become a key factor to optimize product cycles for maximum sustainability and economic performance of the production techniques. Traditionally, light alloys, mainly aluminum ones (2000 and 7000 series), are broadly used in the manufacture of airplanes structural components due to their excellent mechanical properties-weight ratio [1]. In particular, UNS A97075 (Al-Zn) alloy is involved in the production of wings, spar caps and the upper skins [2]. Machining operations are one of the most commonly used to manufacture these components. Despite the frequent use of cutting fluids to improve tool life and functionality of machined parts, the current trend is the application of alternative and more sustainable lubrication strategies, such as Minimum

Quantity Lubrication (*MQL*) or the complete removal of these polluting agents from the production process (dry machining) [3]. Nonetheless, the total absence of cutting fluids in these operations leads to severe conditions which may negatively affects the surface requirements of the manufactured parts. In this sense, surface integrity has become a weighty quality property in aeronautical industry. In general, surface integrity may be referred to as the set of material properties developed or affected subsequently to any forming process. Three approaches may be taken into account for the evaluation of these properties, such as the geometric variables, both at the macroscale (dimensional and geometric deviations) and at the microscale (roughness profile), as well as the physical-chemical and mechanical properties (e.g., residual stresses, microhardness, corrosion resistance and fatigue behavior) [4]. Of the different properties mentioned above, related to surface integrity, fatigue behavior is particularly important due to safety reasons. Usually, fatigue fracture is caused by the sudden decrease of the

stress-bearing section due to the crack growth after the microcracks generation and nucleation [5]. Different studies have been focused on the analysis of the residual stresses, surface roughness, and microstructure influence on fatigue life. Thus, the surface integrity of manufactured components impact on the initial phase of the fatigue fracture is clearly proved [6]. A great variety of models (potential or exponential, among others) may be found in the literature. These models allow obtaining the dependence between the cutting parameters (cutting speed, v_c; feed rate, f; depth of cut, a_p) and several variables of the roughness profile (such as the maximum height of roughness profile, R_z, or the arithmetic average of roughness profile, R_a) [7-8]. Hence, significant research has evinced the feed rate as the most dominant variable on the maximum height of profile regardless the cutting speed and the depth of cut [9]. However, micro-geometric tolerance studies focused on this output estimation are less common as compared to average roughness [10-12]. On the other hand, in the last decade, the rise of automatic learning and artificial intelligence techniques, combined with big data and cloud computing methods, have faced any machining process parameter forecasting efficiently. In this regard, Artificial Neural Networks (*ANN*s) has become one of the most used supervised machine-learning algorithms to model and predict output variables in machining operations [13-14]. In this regard, different works have tried to predict several properties related to surface roughness as a function of cutting parameters for turning operations using *ANN*-based models [15-16].

Nevertheless, the "black box" nature of *ANN*s constitutes a major weakness in contrast with traditional statistical approaches, involving multiples sources of randomness and, therefore, showing problems on the reproducibility of predictions. Thereby, the network performance depends on the heuristic adjustment of numerous hyperparameters (e.g., number of neurons considered in the input, hidden and output layers, activation functions, learning rate, batch size and momentum coefficients, among others). Taking these values adopted by similar works as a reference, an architecture with 1 to 3 hidden layers and a number of neurons between 1 and 20 with a "purelin" function for output layer together with a batch size for training, validation, and test accounting for 70-15-15 (%) respectively of the total data set [17], may be considered initially for the response variable estimation.

Several works have tried to increase the computational performance and accuracy of a predictive model for surface roughness through tuning hyperparameters [18]. In many of them, genetic and metaheuristic algorithms are used to optimize the hyperparameters specially for Convolutional Neural Networks [19]. Thus, maximum accuracy is achieved after modeling several architectures by varying the number of filters, kernel size and number of layers. In addition, some standard strategies rely on grid, random or Bayesian search for this task [20]. This involves, training models with all possible combinations of the selected hyperparameter values, training models with randomly samples hyperparameters values from the defined distribution or starting with an initial guess of values, using performance of the model to the values respectively. However, the approach suggested by many of whom to explore and analyze the influence of control hyperparameters does not study how it affects the distribution of data for each phase. Therefore, in the present work, an analysis of *ANN* application was aimed to predict suitable cutting parameters for maximum height of roughness profile, as a magnitude of surface quality, in the dry turning of UNS A97075 alloy. In this regard, the inputs considered in the regression model were the cutting speed and the feed rate. Additionally, an *ANN* optimization approach was presented to obtain optimal number of neurons in the hidden layer and the batches data ordering with minimal error associated, in order to achieve the best sequencing option.

2. METHODOLOGY

Several dry-turning experiments were carried out to study the cutting parameters effect on roughness profile of the UNS A97075-T6 (Al-Zn) alloy. The specimen geometry is shown in Figure 1. This geometry was selected according to the ISO 1143:2010 standard, used to evaluate

the fatigue behavior. There are three different areas (fixed, calibrated and support zone) characterized by its length (L_z) and respective diameter (D_z).
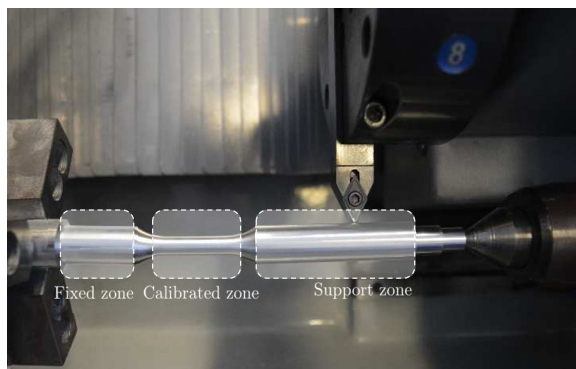
Fig. 1. Zones distinguished in the parallel specimen-single point loading geometry

The selected specimen geometrical dimensions for the areas mentioned are specified in the Table 1.

Table 1

Parallel specimen geometry

Zones	D_z [mm]	L_z [mm]
Fixed	15	30
Calibrated	7.5	25
Support	15	65
Total	-	167

The cutting conditions values employed in the tests are illustrated in the Table 2. The combination of these values gave rise to a finishing step for each turned sample. It is necessary to mention that is not often work with this alloy at low cutting speeds. Nevertheless, these values are very common when it is combined with other materials, such as Titanium alloys or Carbon Fiber Reinforced Polymers (*CFRP*), among others.

Table 2

Cutting parameters

f [mm/rev]	v_c [m/min]	a_p [mm]
0.05	40	
0.10	60	1
0.15		
0.20	80	

The tool used was a rhombic uncoated WC-Co insert, with ISO reference DCGT11T308-14 IC20, in a neutral position (a cutting-edge angle of 62.5 degrees). Following the machining tests, a macro and micro geometrical deviations inspection was conducted. To evaluate surface quality, in terms of the mean roughness depth (R_z), a portable roughness tester (Mitutoyo SURFTEST SJ-210) was employed. For this purpose, four roughness measurements were conducted along four generatrix of the specimen (90º apart). Because of the geometry of the specimens themselves, and related accessibility issues, the roughness profile parameter concerned was measured in the support and fixed zone (Figure 2).

Fig. 2. Roughness measurement system in the fixed zone

A four specimens set was machined for each cutting parameter combination to guarantee a 95% confidence level and a 50% probability of failure under the ISO 12107 standard. Hence, 4 samples test, 12 combinations and 8 repetitions were carried out to assemble a 384 measurements dataset. This sample size may be deemed adequate to define the *ANN* model. On the subject matter of this work, a Single Hidden Layer Feedforward Neural Network (*SLFN*) with two input variables (v_c and f) and one output variable (R_z) was used. For that purpose, the MATLAB Neural Network Toolbox library have been used. Figure 3 shows the network architecture considered based on simple Perceptron, with N as the neurons number in the hidden layer.
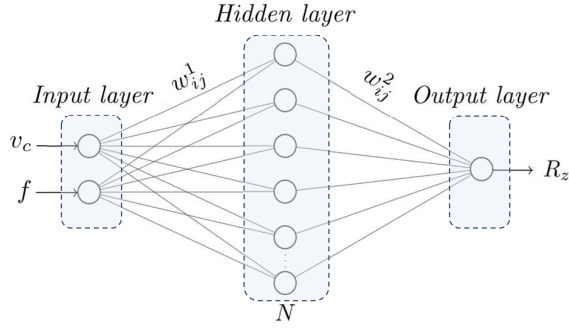
Fig. 3. *ANN* structure used to predict maximum height of roughness profile (R_z) as a function of two features variables (cutting parameters v_c and f)

On the other hand, the Root Mean Square Error (*RMSE*) and the Adjusted *R* squared (R^2) have been used as *ANN* performance measurement as follows (Equations 1-2).

$$RMSE = \sqrt{\frac{1}{T}\sum_{t=1}^{T}(\hat{y}_t - y_t)^2}, \qquad (1)$$

$$R^2 = \frac{\sum_{t=1}^{T}(\hat{y}_t - \bar{y})^2}{\sum_{t=1}^{T}(y_t - \bar{y})^2}, \qquad (2)$$

where $\hat{y}_t$, y_t and $\bar{y}$ are the model computed, measured values of maximum height of roughness profile variable and the mean of y values respectively. In addition, T represents the total of observations. In terms of network topology hyperparameters, the sigmoid transfer function was used. Thus, linear output layer lets the *ANN* produce values inside the range 0 to 1. Furthermore, the Bayesian Regularization backpropagation algorithm was made use of since it is considerably accurate compared to others (e.g., such as Levenberg-Marquardt or Scaled Conjugate Gradient learning algorithms). Likewise, to provide access to each batch, i.e., controlling the amount and selection of data mining sets intended for training, validation and testing tasks, an index data division function was used. Moreover, by storing the weights and biases for the optimal configuration of the *ANN* model (whose configuration for training, validation, testing and number of neurons in the hidden layer minimizes the *RMSE*) makes possible to reduce the network random behavior. Therefore, if *ANN* is run again, similar results should be obtained.

The 70% of the dataset was allocated to training task (267 data). The remaining 30% (117 data) was used to validate (58 data) and test (59 data) the *ANN* model, as well as carry out a final performance evaluation and stop training before overfitting occurs. Finally, according to the methodology proposed, the *ANN* behavior was studied for *N* from 1 to 20 neurons to choose the optimal number of neurons in the hidden layer. After 200 iterations performed, the final *ANN* was trained for a number of hidden layer neurons with minimal mean *RMSE*. The methodology described above may be summarized in the following flowchart.
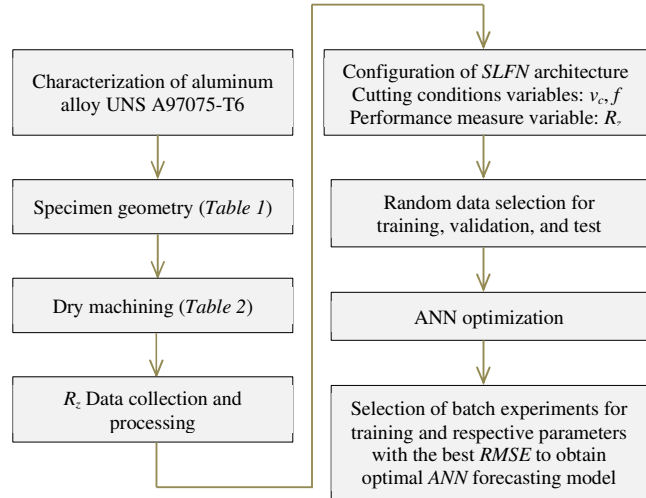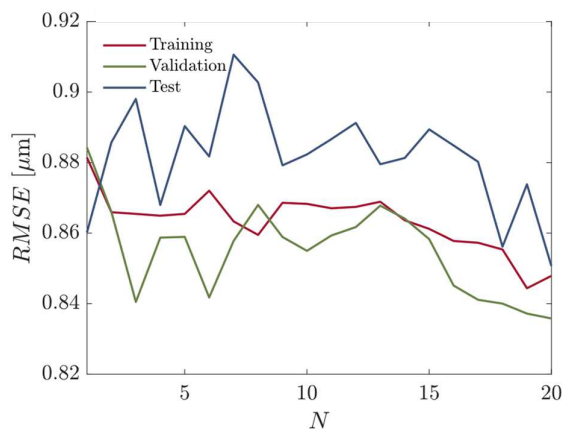

Fig. 4. Flowchart of the methodology used

3. RESULTS AND DISCUSSION

An initial analysis was carried out to determine if it is possible to find a certain correlation between number of the hidden layer neurons (*N*) and global minimum mean error (*RMSE*) data pattern, considering the respective splitting ratio for each phase. Of the total 4000 *ANN*s runed, Figure 4 shows those combinations grouped by common number of hidden neurons (from 1 to 20) in which training phase was stopped due to the minimization of mean *RMSE*. The results revealed major performance enhancements for networks trained with 19 and 20 hidden neurons, i.e., in 35% of cases (70 of 200 iterations), such number of hidden neurons were submitted by the optimal networks (with minimal *RMSE*) tested. Probabilistically, the higher number of neurons, the lower the error
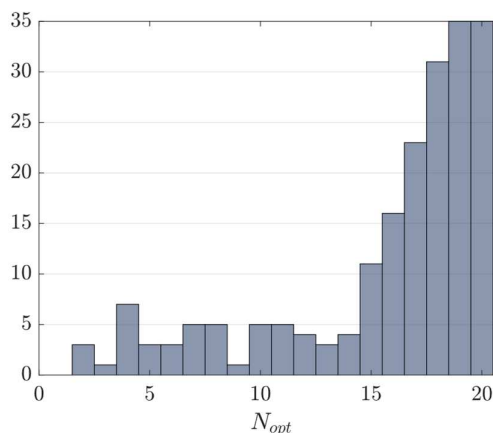
value, since an excessively low number lead to underfitting and high statistical bias. This is consistent with *ANN*s learning method, the more hidden neurons, the more accurate the weighs quantity fitting. Notwithstanding, by increasing the number of neurons further, overfitting and significant execution time may be evidenced, and no improvement is observed in the reduction of error. For the limit of 20 neurons as depicted in Figure 6, this phenomenon does not appear to occur. Besides that, a similar approach was proposed to optimize the number of data values for training, validation, and test. However, no value was clearly found to minimize the error rate and 70-15-15 (%) combination was adopted.

Fig. 6. Histogram for the optimal number of neurons considered in the hidden layer (N_{opt}) to minimize *RMS*

Fig. 5. Root Mean Square Error (*RMSE*) evolution as function of the neurons number in the hidden layer (N)

As it can be observed in Figure 5, the *RMSE* curves reach simultaneously a minimum peak mean error of 0.846 μm for 20 hidden layer neurons, according to the neurons pattern distribution shown in Figure 6. In addition, the validation phase error is lower than the training one and, in turn, this value is less than test task one. Therefore, considering the highest *RMSE* value during the test is achieved for 20 neurons (very close to the validation error), the results obtained shows a good generalization of the model, as the 70% of the randomly selected data for neural network training are considered sufficiently representative of the ANN behavior and it may be considered valid for inference.

The representation of this performance metric provides a simple physical interpretation of the machining target forecasting problem, in accordance with roughness profile

Subsequently, the aim was to store the greatest combinations of data values for training, validation, and test. To that effect, as shown in Table 3, the *RMSE* parameter in each phase is compared for the optimal and worst sets orders.

Table 3

Minimum and maximum values of *RMSE* in the training ($RMSE_{tr}$), validation ($RMSE_v$), and test ($RMSE_t$) phases [μm] with the corresponding number of hidden layer neurons (N)

| N	$RMSE_{tr}$	$RMSE_{val}$	$RMSE_t$
2	0.7295	1.2285	0.8024
6	0.8784	0.9096	0.8984

Thus, the minimum value of total mean *RMSE,* considering the ratios for each task previously mentioned, is 0.8153 μm (for 2 hidden layer neurons) compared with the maximum of 0.8861 μm (for 6 hidden layer neurons). However, this number of hidden neurons (N) contrasts with the value for the highest probabilistic success shown in Figures 5-6 (N_{opt} = 20 neurons). In this context, the need for conducting a thorough analysis seems to be justified. Therefore, the degree of performance is around 8.68% for all networks tested regarding the worst case. On the other hand, Figure 7 shows the *RMSE* results during the *ANN* training ($RMSE_{tr}$). According to Table 3, the level of error concerned with training phase for the lowest total *RMSE* obtained is considerably smaller than the lowest histogram limit shown in Figure 7. According to this figure,

the most repeatable *RMSE* value (about 13% of networks trained) coincides with the upper limit. Similarly, Figure 8 reveals the *RMSE* distribution for the validation phase (*RMSE$_{val}$*). Particularly, the error parameter in validation, corresponding to the minimum global mean error (*RMSE$_{tot}$*), is higher than that associated with maxim total mean one (Table 3).
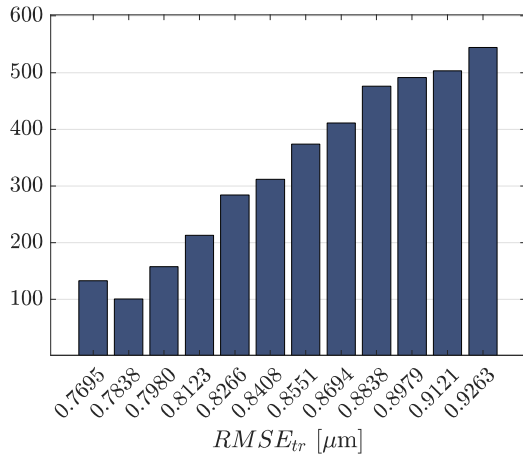
Fig. 7. Frequency distribution of mean Root Mean Square Error for *ANN* training (*RMSE$_{tr}$*)

In this instance, *RMSE$_{val}$* related with minimum *RMSE$_{tot}$* is above the upper limit, whereas *RMSE$_{val}$* for maximum *RMSE$_{tot}$* is close to the most repeated value (about 11% of networks validated). In accordance with this distribution, the most common *RMSE$_{val}$* value (14% of all cases) is over 65% of the *RMSE$_{val}$* with optimal *RMSE$_{tot}$* and a 10% lower than the *RMSE$_{val}$* with worst *RMSE$_{tot}$*.
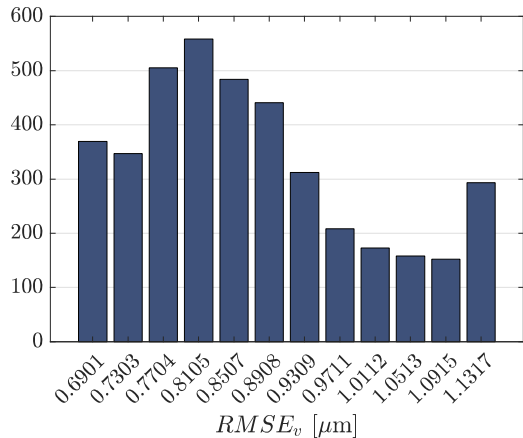
Fig. 8. Frequency distribution of mean Root Mean Square Error for *ANN* validation (*RMSE$_{v}$*)

Likewise, Figure 9 illustrates the mean *RMSE* distribution for the test phase (*RMSE$_{t}$*). By

analyzing the results, values below the minimum *RMSE$_{t}$* are reached on average in 25% of the networks studied, however, errors above the maximum *RMSE$_{t}$* threshold were exceeded at 40% of the total number or *ANN*s.
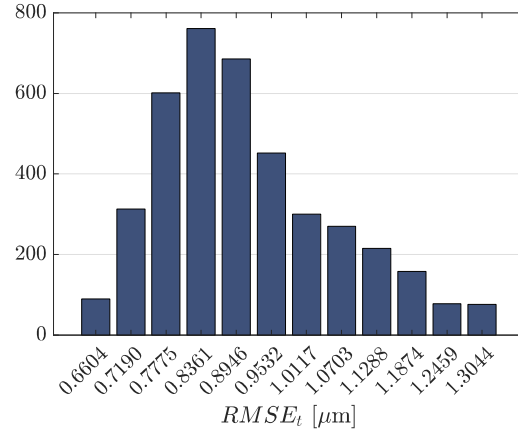

Fig. 9. Frequency distribution of mean Root Mean Square Error for *ANN* test (*RMSE$_{t}$*)

Hence, there are certain dataset values combination for test with an error less than minimal *RMSE$_{t}$*. Moreover, the most likely *RMSE* at test (20% of all networks solved) is occurred for an amount higher than the minimum *RMSE$_{t}$* by 5%. As a weighted sum, Figure 10 shows the mean frequency distribution of total mean root mean square (*RMSE$_{tot}$*).
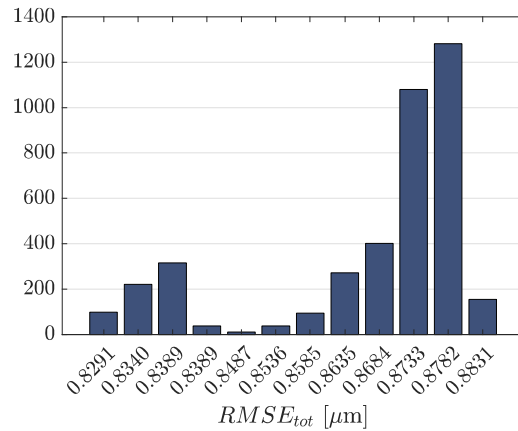
Fig. 10. Frequency distribution of total mean Root Mean Square Error (*RMSE$_{tot}$*)

Considering the most favorable *RMSE$_{tot}$* result obtained from Table 3, it is far below the lower limit exposed in Figure 10. Furthermore, the maximum *RMSE$_{tot}$* value exceeds frequency
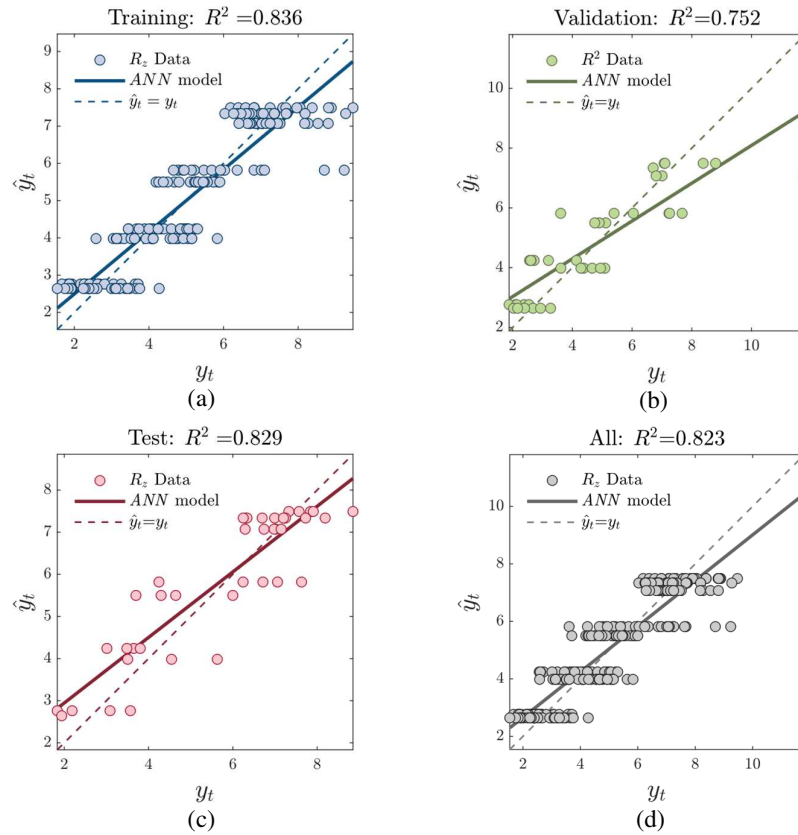
Fig. 11. *ANN* regression-model results. (a) Training data. (b) Validation data. (c) Test data. (d) Complete dataset

histogram limits. Additionally, a considerable part of the results (around 60%) has shown an error value of less than 3% of most the frequent one, while only 5% of data showed an error higher than 0.5%. Consequently, the optimization approach proposed in this work may be considered to improve *RMSE* metric for approximate values constrained between upper and lower graphic bounds. Once the *ANN* topological hyperparameters optimization were carried out, the optimal *ANN* is intended to be worked on. For that purpose, it has been collected the data batches indexes with best *RMSE* performance and the optimal number of neurons in the hidden layer (N_{opt}), previously reported, as well the best weights, and biases values. On the other hand, Figure 10 indicates the best ANN based-linear regression for the training, validation, test, and the complete dataset. The adjusted R-squared (R^2) in the training phase was 0.836 which is slightly higher than the test one, 0.829, whereas the validation

error is the maximum with respect to the above phases, 0.752. This behavior is consistently in good agreement with the Figure 5. Additionally, the R^2 for the complete dataset was 0.823 (Figure 11 (d)). The results reached contrast with other regression models, such as the potential one ($R^2 = 0.711$) and the Response Surface Methodology (*RSM*) analysis ($R^2 = 0.680$). In consequence, an acceptable fit has been obtained by the *ANN* model shown in Figure 3.

As a final result, if the *ANN* is intended to be rerun, its variability behavior is reduced and close output values may be predicted, achieving an enhanced level of accuracy compared with the results obtained probabilistically in most cases. In such a way, the *ANN* optimization has been evidenced to be a valid approach for the micro-geometric variable forecast studied. In addition, Figure 12 shows the predicted values of the maximum height of roughness profile dependent on f, for each v_c. From $f = 0.05$ to 0.10 mm/rev a slightly variation in R_z was observed for both f and v_c parameters.
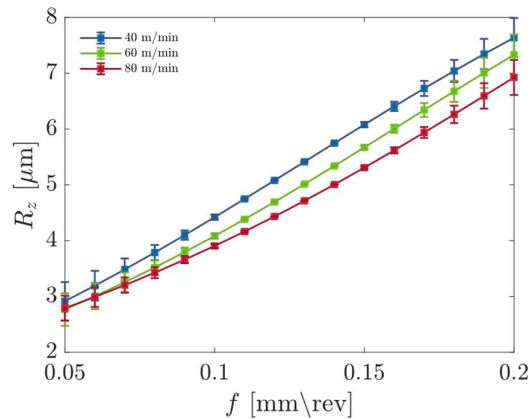
Fig. 12. Mean *ANN* predicted values of the of the maximum height of roughness profile (R_z) as a function of the feed rate (f), for each cutting speed (v_c)

Specifically, for $f = 0.05$ mm/rev, the set of R_z curves obtained for different v_c, are almost identical in R_z forecast. Nevertheless, a major R_z increase was recognized from $f = 0.10$ to 0.20 mm/rev. In addition, for the high level of cutting speed (v_c) considered (80 m/min), the R_z target variable was increased 2.7 times (from 2.8 to 7.6 µm). In contrast, the increment was lower for medium and low range (40-60 m/min), where the R_z target variable was increased 2.5 times (from 2.8-2.9 to 6.9-7.3 µm). Besides that, there is an observed trend indicating that higher cutting speeds correspond to reduced R_z values. Thus, according to the literature [9], f feature appears to be the most influential cutting parameter. Besides this, the R_z value showed a consistent trend to grow with f, mostly from $f = 0.10$ mm/rev. Notwithstanding, vc showed a lighter influence, becoming most appreciable for high values of f (from $f = 0.10$ mm/rev). As it could be expected, all of these observations are consistent with literature works about dry machining of aluminum alloys [10-12]. Moreover, according to the error bars corresponding to the standard deviation for each predictive *ANN* point, a robust behavior is observed for f values ranging from 0.07 to 0.17 mm/rev (bigger dataset size is available) compared to the upper and lower extremes, where the prediction error tends to increase.

4. CONCLUSIONS

In this work, a sigmoid transfer function in the hidden layer and the Bayesian Regularization training algorithm were used as *SLFN* hypermeters to predict maximum height of roughness profile of UNS A97075 dry turned specimens. Among the *ANN*s executed with random combinations of data batches intended for training (70%), validation (15%) and test (15%), the optimal number of neurons in the hidden layer (N_{opt}) was 20, which resulted in the lowest *RMSE* level.

The mean *RMSE* for all data set was about $\pm 15\%$. This translates into an enhancement level of 8.68% regarding the network with the highest error. Although the improvement in predictive quality is relatively low, it can be increased with the number of neural networks tested. In terms of *RMSE* magnitude for the most desirable *ANN* during the training and test phases, the results obtained were considerably smaller than the lower limits for the mean value in both cases. However, the *RMSE* determined for validation task exceeded even the upper limit of the corresponding mean error, therefore, there is scope for accuracy improvement by increasing the number of *ANN*s implemented and exploring other combinations.

Consequently, the model training gave rise to acceptable fit, showing a coefficient of determination (R^2) for all dataset of 0.823. This goodness-of-fit has been compared with other regression models like potential and *RSM* analysis by evidencing the best fit for both of them. Thus, the application of a shallow *ANN* has proved to be a useful instrument for obtaining a R_z predictive model, as a function of v_c and f under the cutting conditions described above.

Furthermore, the network optimization approach presented in this work, improves the prediction performance, provide insight into the *ANN* architecture parameters, and limits the random behavior of the algorithm.

5. ADKWNOLEGMENTS

6. REFERENCES

[1] Alba-Galvín, J, González-Rovira, L., Bethencourt, M, Botana, F., Sánchez-Amaya, J. *Influence of Aerospace Standard Surface Pretreatment on the Intermetallic Phases and CeCC of 2024-T3 Al-Cu Alloy*, Metals, 2019, 9, 320, https://doi.org/10.3390/met9030320

[2] Goncharenko, A. V. *Aeronautical and aerospace material and structural damages to failures: theoretical concepts*, Int. Journal of Aerospace Engineering, 2018, pp. 1-7, https://doi.org/10.1155/2018/4126085

[3] Krolczyk, G. M., Maruda, R. W., Krolczyk, J. B., Wojciechowski, S., Mia, M., Nieslony, P., & Budzik, G. *Ecological trends in machining as a key factor in sustainable production– A review*, Journal of Cleaner Production, 2019, 218, pp. 601-615, https://doi.org/10.1016/j.jclepro.2019.02.017

[4] M'saoubi, R., Outeiro, J. C., Chandrasekaran, O. W., Dillon Jr, Jawahir, I. S. *A review of surface integrity in machining and its impact on functional performance and life of machined products*, International J. of Sustainabl.Manuf.,2008, 1(1-2), pp. 203-236, https://doi.org/10.1504/IJSM.2008.019234

[5] Schijve, Jaap (eds). *Fatigue Crack Growth. Analysis and Predictions*, Fatigue of Struct. and Materials, Springer, Dordrecht, 2009, pp. 209-256, https://doi.org/10.1007/978-1-4020-6808-9_8

[6] Matsumoto, Y., Hashimoto, F., & Lahoti, G. *Surface integrity generated by precision hard turning*, CIRP Annals, 1999, 48(1), pp. 59-62, https://doi.org/10.1016/S0007-8506(07)63131-X

[7] Salguero, J., Puerta, F. J., Gomez-Parra, A., Trujillo, F. J., Sevilla, L., & Marcos, M. *An analysis of geometrical models for evaluating the influence of feed rate on the roughness of dry turned UNS A92050 (Al-Cu-Li) alloy*, Advances in Materials and Processing Technologies, 2016, 2(4), pp. 578-589, https://doi.org/10.1080/2374068X.2016.1247333

[8] Martín Béjar, S., Trujillo Vilches, F. J., Bermudo Gamboa, C., & Sevilla Hurtado, L. *Fatigue behavior parametric analysis of dry machined UNS A97075 aluminum alloy*, Metals, 2020, 10(5), 631, https://doi.org/10.3390/met10050631

[9] Horváth, R., & Dregelyi-Kiss, A. *Analysis of surface roughness of aluminum alloys fine turned: United phenomenological models and multi-performance optimization*, Measurement, 2015, 65, pp. 181-192, https://doi.org/10.1016/j.measurement.2015.01.013

[10] Torres, A., Puertas, I., & Luis, C. J. *Surface roughness analysis on the dry turning of an Al-Cu alloy*, Procedia engineering, 2015, 132, pp. 537-544, https://doi.org/10.1016/j.proeng.2015.12.530

[11] Trujillo Vilches, F. J., Marcos Bárcena, M., & Sevilla, L. *Experimental prediction model for roughness in the turning of UNS A97075 alloys*, Materials Science Forum, 2014, 797, Trans Tech Publications Ltd, pp. 59-64, https://doi.org/10.4028/www.scientific.net/msf.797.59

[12] Benardos, P. G., & Vosniakos, G. C. *Predicting surface roughness in machining: a review*, International Journal of Machine Tools and Manufacture, 2003, 43(8), pp.

833-844, https://doi.org/10.1016/S0890-6955(03)00059-2

[13] Jurkovic, Z., Cukor, G., Brezocnik, M., & Brajkovic, T., *A comparison of machine learning methods for cutting parameters prediction in high-speed turning process*, Journal of Intelligent Manufacturing, 2018, 29, pp. 1683-1693, https://doi.org/10.1007/s10845-016-1206-1

[14] K. Dong-Hyeon et al., *Smart Machining Process Using Machine Learning: A review and Perspective on Machining Industry*, International Journal of Precision Engineering and Manufacturing-Green Technology, 5, pp. 555-568, 2018, https://doi.org/10.1007/s40684-018-0057-y

[15] A. Kohli and U. S. Dixit, *A neural-network-based methodology for the prediction of surface roughness in a turning process*, The International Journal of Advanced Manufacturing Technology 25, pp. 118-129, 2005, https://doi.org/10.1007/s00170-003-1810-z

[16] Durmus Karayel, *Prediction and control of surface roughness in CNC lathe using artificial neural network*, Journal of Materials Processing Technology, Volume 209, Issue 7, 2009, pp. 3125-3137, https://doi.org/10.1016/j.jmatprotec.2008.07.023

[17] Mia, M., & Dhar, N.R, *Prediction of surface in hard turning under high pressure coolant using Artificial Neural Network*, Measurement, 92, 2016, pp. 464-474, https://doi.org/10.1016/j.measurement.2016.06.048

[18] Arapoğlu, R. A. et al., *An ANN-based method to predict surface roughness in turning operations*, Arab J Sci Eng, 42, 2007, pp. 1929-1940, https://doi.org/10.1007/s13369-016-2385-y

[19] Loussaief, S., & Abdelkrim, A., *Convolutional neural network hyper-parameters optimization based on genetic algorithms*, International Journal of Advanced Computer Science and Applications, 9(10), 2018, http://dx.doi.org/10.14569/IJACSA.2018.091031

[20] Alibrahim, H., & Ludwig, S. A., *Hyperparameter optimization: Comparing genetic algorithm against grid search and bayesian optimization*, IEEE Congress on Evolutionary Computation (CEC), 2021, pp. 1551-1559, http://doi.org/10.1109/CEC45853.2021.9504761

Optimizarea rețelei neurale artificiale pentru predicția rugozității suprafeței la strunjirea uscată a aliajului de aluminiu A97075

Lucrarea prezintă modelul de predicție a rugozității suprafeței la strunjirea uscată a aliajului de aluminiu aeronautic UNS A97075 utilizând rețeaua neuronală artificială (ANN). În mod specific, impactul vitezei de tăiere și al vitezei de avans asupra înălțimii maxime a profilului de rugozitate au fost analizate în raport cu influența sale asupra comportamentului la oboseală a pieselor prelucrate. Efectul arhitecturii rețelei, cum ar fi numărul optim de neuroni din stratul limită și numărul de rezultate experimentale aplicate pentru validarea experimentelor, a fost studiat pentru a determina modelul de regresie cu cea mai mare acuratețe de predicție și minimizarea erorilor. Rezultatele raportate au arătat o potrivire bună în modelul prelucrat.

Ignacio REPISO-LÓPEZ, Research Assistant, Department of Civil, Materials and Manufacturing Engineering, EII, University of Malaga, C/Dr, Ortiz Ramos s/n, E-29071 Malaga, Spain, irepiso@uma.es

Sergio MARTÍN-BÉJAR, PhD Lecturer, Department of Civil, Materials and Manufacturing Engineering, EII, University of Malaga, C/Dr, Ortiz Ramos s/n, E-29071 Malaga, Spain, smartinb@uma.es

Francisco Javier TRUJILLO-VILCHES, PhD Lecturer, Department of Civil, Materials and Manufacturing Engineering, EII, University of Malaga, C/Dr, Ortiz Ramos s/n, E-29071 Malaga, Spain, trujillov@uma.es

Lorenzo SEVILLA-HURTADO, PhD Senior Lecturer, Department of Civil, Materials and Manufacturing Engineering, EII, University of Malaga, C/Dr, Ortiz Ramos s/n, E-29071 Malaga, Spain, lsevilla@uma.es